Research Article

Khalid Mutashar Abed, Nabaa S. Radhi, Ahlam Hamid Jasim, Zainab S. Al-Khafaji*, Sabaa Radhi and Safa A. Hussien

Study the effect of adding zirconia particles to nickel–phosphorus electroless coatings as product innovation on stainless steel substrate

https://doi.org/10.1515/eng-2022-0364
received April 19, 2022; accepted August 01, 2022

Abstract: Scholars have spent much time studying metal deposition procedures involving the deposition of electroless nickel, alloy, and composite coatings on various surfaces; the most current uses were feasible advantages of the coatings' many good properties for achieving the final product innovation. Lately, these coatings have demonstrated intriguing wear and corrosion resistance features, resulting in several innovative macro-level developments. The notion of composite coating by co-deposition coating has been presented in this article. The characteristics of Ni–Pb alloy coatings were examined by inserting particles into the electroless deposited solution. The stainless steel (SS) specimens have been electroless coated with Ni–Pb and ZrO_2 nanoparticles (size = 30–70 nm) at 0, 10, and 20 g/L amounts. The materials have been examined using scanning electron microscope and atomic force microscope, followed by wear-resistant and microhardness testing. According to the investigation findings, including inert particles improved the hardness magnitude and wearing resistance considerably. The base metal exhibited the highest wear rate at 10 N, while the-wear rate decreased in the Ni–Pb–ZrO_2-coated SS316L by 34%. The Vickers hardness magnitudes of the Ni–Pb–ZrO_2-coated samples at different ZrO_2 contents (0, 10, and 20 g/L) were 19, 50, and 81%, respectively.

Keywords: composite coating, electroless nickel–phosphorus, product innovation, stainless-steel, zirconia, wear-resistant, micro-hardness test

1 Introduction

Electroplating is commonly considered the traditional electrolytic plating process. It is achieved when metal ions are first reduced to their respective metallic states before deposition at the cathode under an external electrical source [1]. Electroless plating can be likened to a chemical reduction process in many aspects, even though they differ significantly. It includes the catalytic decrease of metallic ions in a reducing agent-containing aqueous solution, followed by the subsequent deposition of the metal without any external energy source [2–7].

Electroless Ni–P/Ni–B coatings offer a wide range of applications in sectors that demand high hardness and anti-corrosion rates. The reason for such a thin layer of deposition is that the activated surface seems to be no longer in touch with the electroless solution after the metal is deposited. Because the deposited metal is in touch with the bath, no additional reaction can occur. As a result, at such a thin deposition thickness, it is critical to keep the surface roughness to a minimum, as this characteristic of the coating is linked to other characteristics, including wear and friction that also decrease coating life by subjecting the substrate to increased wear and corrosion, thereby increasing the price.

The chemical nickel reductions result in the formation of the electroless nickel deposit; however, this process depends on the reducing agent utilized. For instance, nickel-phosphorus coatings are produced when hypophosphite is utilized as the reducing agent [8]. Hence, the reaction must be controlled to ensure the reduction only

* **Corresponding author: Zainab S. Al-Khafaji,** Department of Civil Engineering, Universiti Kebangsaan Malaysia, 43600 Bangi, Selangor, Malaysia, e-mail: p123005@siswa.ukm.edu.my
Khalid Mutashar Abed, Nabaa S. Radhi: Metallurgical Engineering Department, College of Materials Engineering, University of Babylon, Babil, Iraq
Ahlam Hamid Jasim: Department of Water Resources Management Engineering, College of Engineering, Al-Qasim Green University, Babylon, Iraq
Sabaa Radhi: Mechanical Engineering Department, Altinbas University, İstanbul, Turkey; Al-Turath University College, Baghdad, Iraq
Safa A. Hussien: Building and Construction Engineering Technology Department, AL-Mustaqbal University College, Babylon, Iraq

on the substrate without affecting the equipment utilized. This mechanism can be controlled by adding additives to the reaction baths; such additives may include complexing agents, stabilizers, and pH regulators. Stabilizers are commonly utilized additives when working under stable and adequate conditions for long periods [9,10]. Electroless composite coatings are used to co-deposit composite substrates utilizing electroless coatings. Resistance against wear composites may be created by the co-depositions of small particulate substrates; studies have documented the co-depositions of hard particles like diamond and silicon carbide as well as solid lubricants such as polytetrafluoroethylene (PTFE) particles [11–14]. Nevertheless, the increased surface area loading of the bath caused by the dispersion of the small particles – which was around 700–800 times more than the standard bath – led to the failure of early efforts at electroless composite coatings and frequently to bath disintegration. However, it has been possible to prepare electroless nickel composite coating using the appropriate stabilizers. Electroless coating permits accurate surface regeneration and prevents subsequent mechanical finishing [15,16].

The development of electroless coatings relies on the settling and effect of particles on the workpiece surface, followed by the deposition of Ni–P matrix, which will surround these particles. No molecular bonding exists between the introduced fine particles and the metal matrix. Guglielmi [17] has suggested a mathematical model for composite coating electrodeposition. The outcome of the experiments agreed with the proposed mechanism by ref. [17]. Furthermore, Grosjean et al. [18] reported an experimental set-up for electroless Ni-SiC composite coatings production; the study relied on the agitation induced by the circulating fluid. The bath circulation (top to bottom) generated a laminar fluid flow on the sample surface; this type of cell provided the agitation, and one of its advantages is that the particles are kept in suspension within the solution.

Another study by Apachitei et al. [19] demonstrated that Al_2O_3 particles (spherical shaped) exhibited better incorporation compared to irregularly shaped ones; the shape of the particle also determines the kind of deposit's finish. Large angular and small rounded particles normally give rough and smooth surfaces, respectively. Many authors have investigated particles such as SiC, CrC, ZrO_2, Al_2O_3, PTFE, and graphite [20–22].

Nanosized diamond particles (0.52–2.21 wt%) have exhibited a surface change from bright and smooth to foggy and rough appearance with the nodular surface in the electroless Ni–Pb matrix [23]. Another study reported obtaining Ni–Pb composite coatings via the introduction of SiC and Si_3N_4 to investigate their influence on the coating properties and the co-deposition process. The study noted modifications in the mechanism of growth of the metallic matrix by the nanosized particles compared to the nanosized ones [24].

In this work, the aim is to investigate the impact of the introduced ZrO_2 particles with nano-size on the structural and mechanical characteristics of the product in comparison to stainless steel (SS) 316L substrate.

2 Experimental work

2.1 Electroless procedures

Table 1 demonstrates the chemical analysis of the SS316L sample utilized in this study. The sample was chemically analyzed utilizing a device of spectroscopy for metal materials.

All the samples for the experiments were cylindrical, while the final samples were disc-shaped, with thickness = 3 mm, diameter = 12 mm, and surface area = 3.391.

The preparation of the surface of the sample was done by:

(1) First pulverizing the sample surface with Grit silicon carbide papers of different grades (220, 240, 400, 600, 800, 1,000, and 1,200), followed by surface cleaning with brine and acid; the cleaning process was done in preparation for the electroless process based on the required period per sample.
(2) Then the surface was then pretreated for substrate deposition; the substrates were first cleaned with NaOH (10%) for 10–20 min at 60–80 °C to clean off grease, then it was rinsed with water and dipped in HCl (5%) for 30 s for surface activation before rinsing in deionized water before electroless [25].

Table 1: Chemical analysis of the specimen utilized

Elements	C	Si	Mn	P	Cr	Mo	Ni	Al	Cu	Fe
Percentage × 10^{-2}%	1.9	44.2	85.4	4.6	1,671	209	1,007	0.12	35.6	Rem

(3) Table 2 presents the chemical composition and operating conditions of the plating baths. The deposition process was conducted in a 150 mL bath maintained at 90 ± 1°C for 80 min. NaOH was utilized to regulate the pH of the solution to 5. The particles have been prevented from sedimentation by utilizing a magnetic stirrer at 300 rpm as a rotation rate. The samples after the coating process are shown in Figure 1.

The schematic diagram and the electroless set-up utilized in this work are demonstrated in Figure 2. A thermometer has been placed into the electroless plating bath to monitor the temperature of the plating bath. After cleaning and activation, the substrate was immersed in the electroless bath using an inert rod or thread. The substrates have been immersed in the plating bath for a set amount of time to achieve a coating thickness of 30 nm or more. The needed plating time was maintained depending on the plating rate to guarantee the correct plating thickness was reached. The coatings have been rinsed in deionized water and dried in the air after plating. The same procedure was performed for all electroless Ni–Pb and Ni–Pb–ZrO_2 (10 and 20 g/L) alloy coatings to guarantee homogeneous substrate coatings.

2.2 Tests

For evaluating the performance of the coating layers in this research, the following tests were carried out.

2.2.1 Thickness test

The thickness of the Ni–Pb, Ni–Pb–10ZrO_2, and Ni–Pb–20ZrO_2 layer was measured using a thickness measuring device.

2.2.2 Scanning electron microscope (SEM)

Some grain boundary characteristics have been measured by identifying and measuring the phases, shape, and grain size. Moreover, each of these parameters has a

Table 2: Components of an electroless solution [25]

Solution	Chemical composition for 150 mL	Condition of deposition
Ni–Pb solution	Nickel sulfate = 30 g/L Sodium hypophosphite = 25 g/L Sodium citrate = 20 g/L Thiourea = 2 mg/L ZrO_2 = 0, 10, and 20 g/L Nanoscale, *d* (30–70) nm	pH = 5 Temperature = 90 ± 1°C Coating time = 80 min bath stirring rate 300 rpm

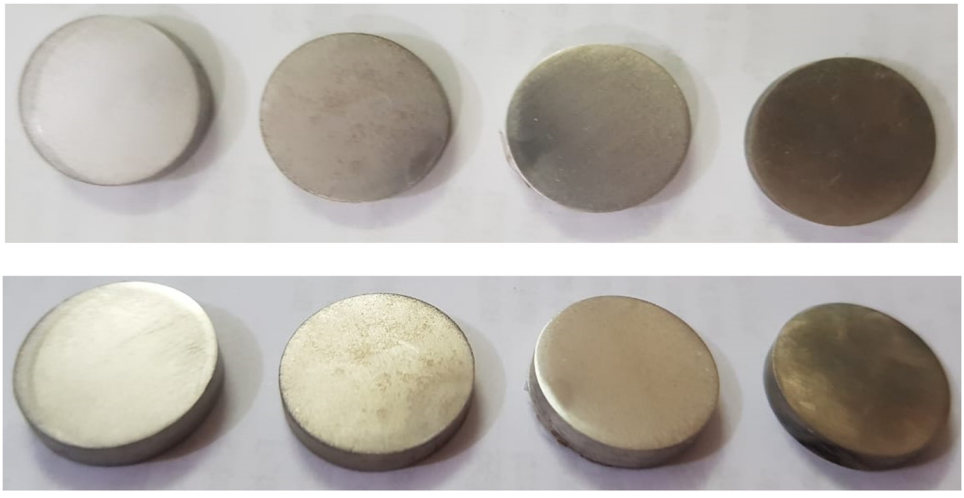

Figure 1: The samples after the coating process.

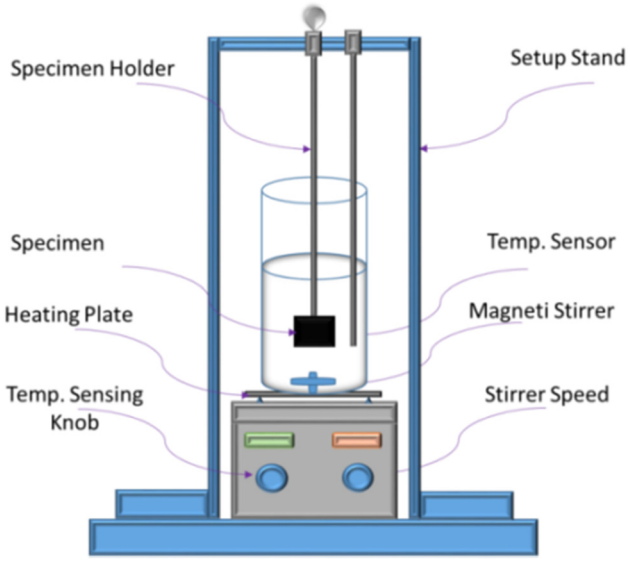

Figure 2: The apparatus of the electroless coating process.

specific characteristic. The Ni–Pb, Ni–Pb–10ZrO_2, and Ni–Pb–20ZrO_2 layers' microstructure were evaluated using contact mode SEM at 2.50k× magnification.

2.2.3 Atomic force microscope

The morphology (films' depth morphology and roughness) of Ni–Pb, Ni–Pb–10ZrO_2, and Ni–Pb–20ZrO_2 layers was observed using atomic force microscopy (AFM, contacting phase, spm AA3000 Angstrom advance Inc., America).

2.2.4 Hardness test

The hardness of the Ni–Pb, Ni–Pb–10ZrO_2, and Ni–Pb–20ZrO_2 layers was measured using TH-717 Digital Micro Vickers Hardness Tester at 200 N load and 20 s holding time.

2.2.5 Wear resistance test

The SS, Ni–Pb, Ni–Pb–10ZrO_2, and Ni–Pb–20ZrO_2 samples have been prepared with a diameter of 12 mm and a thickness of 3 mm following ASTM (G99-04) guidelines [26]. A sensitive electric balancing model with $+0.1 \times 10^{-4}$ accuracy has been utilized to calculate the weight of the specimens. The pin-on-disk idea has been employed to examine dry wear on the wear tester gadget. The specimens have been pressed vs. a standard rotating steel disk with a hardness of 850 HV (in which normal force on the pin (F) = 10 N, pin diameter (d) = 1 cm, disk diameter (d) = 3 cm, wear track radius (R) = 0.5 cm, and disk rotation speed (ω) = 300 rpm). The animals' reduced weight was calculated by weighing them after 5, 10, 15, and 20 min. The following formula has been utilized to transform weight loss into volume loss:

$$\text{Volume loss } (\text{mm}^3) = \frac{\text{Weight loss (g)}}{\text{Density}\left(\frac{\text{g}}{\text{mm}^3}\right)}, \quad (1)$$

where loss in weight = weighting before the test – weighting after the test.

3 Results and discussion

3.1 Thickness results

The observed loss in weight has been converted to loss in volume using the next relation: The thickness of the coating specimens was 30.7 nm for Ni–Pb, 34.5 nm for Ni–Pb-10ZrO_2, and 37.9 nm for Ni–Pb-20ZrO_2, demonstrating that the last coating layers' rates of deposit were great. The reason for this observation could be the ZrO_2-induced high diffusivity of the specimens, as the rate of thickness was found to improve with increases in the particle size and amount of the ZrO_2 layer (Table 3).

3.2 SEM

The SEM micrographs of the specimens at various zirconia contents are demonstrated in Figure 3. The figure also demonstrated the influence of the ZrO_2 content on the coatings' thickness. ZrO_2 particles were deposited in clusters resembling an aggregated base metal composition.

3.3 AFM

The topography of the coating thickness layer for the samples was determined using the AFM, as demonstrated in Figure 4a–c. The figures demonstrated the smooth

Table 3: The thickness of layer coating

Samples	Thickness (nm)
Ni–Pb	30.7
Ni–Pb–10ZrO_2	34.5
Ni–Pb–20ZrO_2	37.9

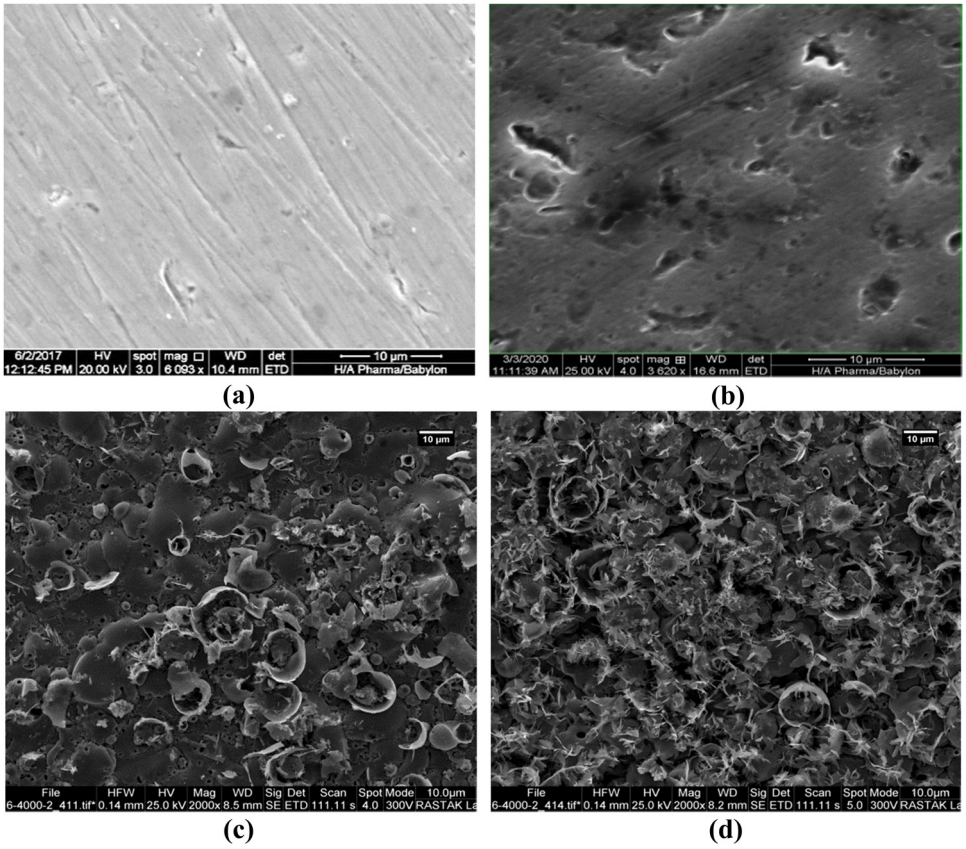

Figure 3: SEM morphology topographic for coating layers at magnification (2,500×): (a) SS, (b) Ni–Pb, (c) Ni–Pb–10ZrO_2, (d) Ni–Pb–20ZrO_2.

morphology of the zirconia layer at 0 g/L (Figure 4a); however, the morphology was less smooth for Ni–Pb upon adding 10 and 20 g/L of nano-ZrO_2 (Figure 4b and c).

3.4 Hardness results

The effect of Ni–Pb, Ni–Pb-10ZrO_2, and Ni–Pb-20ZrO_2 coatings on the hardness magnitude of the base metal was determined using the hardness test. The test also aimed to determine the effect of different ZrO_2 and nickel contents on the hardness magnitudes of the base metal and the coatings. The findings of the hardness test for the base metal and the coatings are presented in Figure 5. The hardness magnitude between the coatings differed due to the different zirconia contents in the layers. The particle size exerted a significant effect on the material hardness, as could be mathematically explicated using the Hall-Petch correlation [27]:

$$\mathrm{HV} = H_0 + K/\sqrt{d}, \tag{2}$$

wher HV is the material's hardness with small granular size; H_0 is the material's hardness is multi-size granular (polycrystalline grain size); K is the constant that represents the slope of the Hv hardness once plotted depending on the material type, and $1/\sqrt{d}$ is the particle's diameter.

The Hall-Petch correlation is a theory that describes the reason for the high hardness magnitudes (520 Hv) of ultra-fine microstructures compared to the coarser particles of the same hardened material.

3.5 Wear tests

The loss in weight of each sample has been converted to the respective density, and the outcomes of this test under the same situations earlier mentioned are presented in Figure 6 previously (F: 10 N); ω: 300 rpm; t: 5, 10, 15, and 20 min.

This study's optimum thickness (37.9 nm) was more than the deposited layer thickness. A layer thickness of <20 nm is considered non-protective.

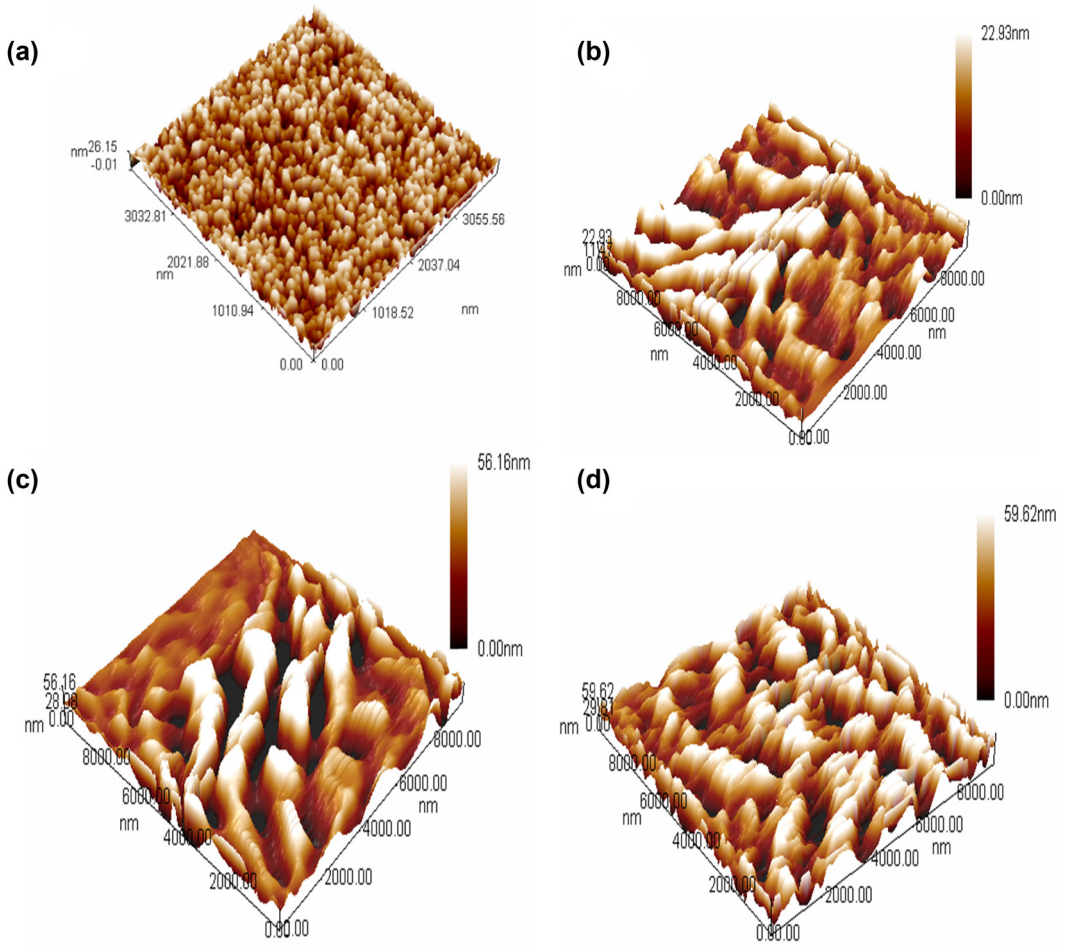

Figure 4: AFM pattern of a sample: (a) SS, (b) Ni–Pb, (c) Ni–Pb-10ZrO_2, (d) Ni–Pb-20ZrO_2.

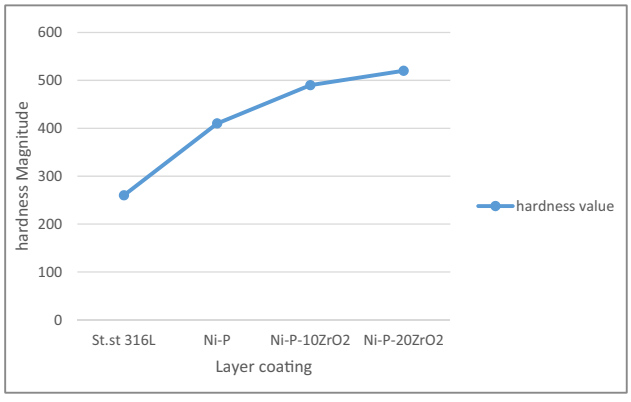

Figure 5: The hardness magnitude for the coated layers.

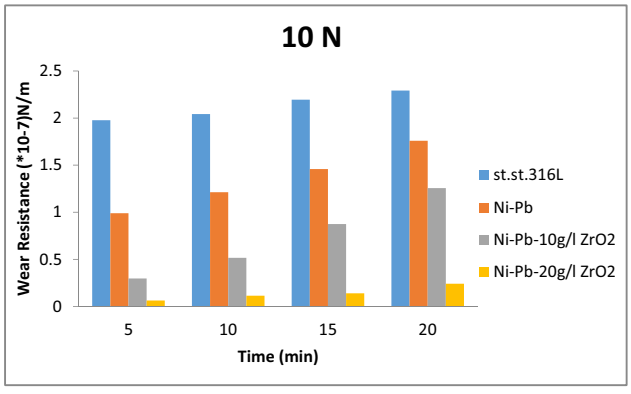

Figure 6: Wear rate of samples at 10 N loads.

Figure 6 demonstrated that the wear rate continued to increase with load magnitudes at a constant velocity due to an increasing rate of sub-surface deformation. This was supported by the results of ref. [28], which found that wear rate increases linearly at a higher sliding distance. The study found that Ni coatings exhibited the most improved properties (in terms of better strength, higher wear, better adhesion, and better corrosion resistance) compared to the properties of the conventional coarse-crystalline coatings.

The results also demonstrated an increase in the volume loss with time due to the increase in particle

loss at prolonged friction time. The effect of adding zirconia particles to the electroless-deposition solution on the wear rates was also studied under different conditions. The results demonstrated a significant reduction in volume loss as the zirconia content increases, reaching the minimum magnitude at the zirconia amount of 20 g/L due to the role of ZrO_2 in increasing the hardness of the coated layers, thereby increasing the wear resistance. The thick layers could be due to the defects and loss of adhesion observed in the coated layer with 10 g/L ZrO_2 after 15 min.

4 Conclusion

The following points are concluded from the test results of the research:

(1) All the coatings demonstrated that the Ni–Pb and Ni–Pb–ZrO_2 composite coatings are completely covered by nanoparticles of about 30–70 nm average grain size.
(2) Ni–Pb–ZrO_2 composite layer demonstrated a stable structure with a good level of crystallization and surface mechanical bonding due to the good interaction between ZrO_2 and the Ni–Pb matrix.
(3) The base metal exhibited the highest wear rate at 10 N, while the wear rate decreased in the Ni–Pb–ZrO_2-coated SS316L by 34%.
(4) The Vickers hardness magnitudes of the Ni–Pb–ZrO_2 coated samples at different ZrO_2 contents (0, 10, and 20 g/L) were 19, 50, and 81%, respectively.

Acknowledgment: The Ministry of Higher Education, University of Babylon, and Al-Mustaqbal University College are gratefully acknowledged. This research was carried out in the laboratory at the University of Babylon.

Conflict of interest: Authors state no conflict of interest.

References

[1] Brenner A, Riddell GE. Electroless plating by a process of controlled self continuing reduction. Proc Amer Eletropl Soc. 1946;33:16.
[2] Brenner A. Nickel plating on steel by chemical reduction. J Res NBS. 1946;37:31–4.
[3] Radhi NS, Al-Khafaji Z. Investigation biomedical corrosion of implant alloys in physiological environment. Int J Mech Production Eng Res Develop. 2018;8(4):247–56.
[4] AbedJanabi ZM, JaberAlsalami HS, Al-Khafaji ZS, Hussien SA. Increasing of the corrosion resistance by preparing the trivalent nickel complex. Egyptian J Chem. 2022;65(6):193–8.
[5] Al-khafaji ZS, Radhi NS, Mohson SA. Preparation and modelling of composite materials (polyester-alumina) as implant in human body. Int J Mech Eng Technol. 2018;9(4):468–78.
[6] Radhi SS, Al-khafaji ZS, Falah MW. Sustainable heating system by infrared radiators. Heritage Sustainable Development. 2022;4(1):42–52.
[7] Radhi NS, Sahi NM, Al-Khafaji Z. Investigation mechanical and biological properties of hybrid PMMA composite materials as prosthesis complete denture. Egyptian J Chem. 2022;65(10):681–8.
[8] Domenech SC, Lima E, Drago V, De Lima JC, Borges NG, Avila AOV, et al. Electroless plating of nickel phosphorous on surface-modified poly(ethylene terephthalate) films. Applied Surface Sci. 2003;220(1–4):238–50. doi: 10.1016/s0169-4332(03)00815-8.
[9] Al-Zubaidy B, Radhi NS, Al-Khafaji ZS. Study the effect of thermal impact on the modelling of (titanium-titania) functionally graded materials by using finite element analysis. Int J Mech Eng Tech. 2019;1:776–84.
[10] Mallory GO, Hajdu JB. Electroless plating: fundamentals and applications. UK: Cambridge University Press; 1990.
[11] Al-Mimar HS, Awadh SM, Al-Yaseri AA, Yaseen ZM. Sedimentary units-layering system and depositional model of the carbonate Mishrif reservoir in Rumaila oilfield, Southern Iraq. Modeling Earth Systems Environment. 2018;4(4):1449–65. doi: 10.1007/s40808-018-0510-5.
[12] Balaraju J, Sankara Narayanan T, Seshadri S. Electroless Ni-P composite coatings. J Appl Electrochem. 2003;33(9):807–16.
[13] Radhi NS. Preparation, characterization, and modeling functionally graded materials in bio-application. PhD thesis. Iraq: University of Technology; 2015.
[14] Yaseen ZM, Aldlemy MS, Oukati Sadegh M. Non-gradient probabilistic Gaussian global-best harmony search optimization for first-order reliability method. Eng Comput. 2019;36(4):1189–200. doi: 10.1007/s00366-019-00756-7.
[15] Agarwala RC, Agarwala V. Electroless alloy/composite coatings: a review. Sadhana. 2003;28(3–4):475–93.
[16] Sahoo P, Das SK. Tribology of electroless nickel coatings: a review. Materials Design. 2011;32(4):1760–75.
[17] Guglielmi N. Kinetics of the deposition of inert particles from electrolytic baths. J Electrochem Soc. 1972;119(8):1009. doi: 10.1149/1.2404383.
[18] Grosjean A, Rezrazi M, Berçot P. Some morphological characteristics of the incorporation of silicon carbide (SiC) particles into electroless nickel deposits. Surface Coatings Tech. 2000;130(2–3):252–6. doi: 10.1016/s0257-8972(00)00714-3.
[19] Apachitei I, Duszczyk J, Katgerman L, Overkamp PJB. Electroless Ni-P composite coatings: the effect of heat treatment on the microhardness of substrate and coating. Scripta Materialia. 1998;38(9):1347–53. doi: 10.1016/s1359-6462(98)00054-2.
[20] Dawood NM, Radhi NS, Al-Khafaji ZS. Investigation corrosion and wear behavior of Nickel-Nano silicon carbide on

stainless steel 316L. Materials Sci Forum. 2020;1002:33–43. doi: 10.4028/www.scientific.net/msf.1002.33.
[21] Grosjean A, Rezrazi M, Takadoum J, Berçot J. Hardness, friction and wear characteristics of nickel-SiC electroless composite deposits. Surface Coatings Technol. 2001;137(1):92–6. doi: 10.1016/s0257-8972(00)01088-4.
[22] Li Y. Investigation of electroless Ni-P-SiC composite coatings. Plating surface Finishing. 1997;84(11):77–81.
[23] Xiang Y, Zhang J, Jin C. Study of electroless NI-P Nan-meter diamond composite coatings. Plating Surface Finishing. 2001;88(2):64–7.
[24] Sarret M, Muuuller C, Amell A. Electroless NiP micro- and nano-composite coatings. Surface Coatings Techn. 2006;201(1–2):389–95. doi: 10.1016/j.surfcoat.2005.11.127.
[25] Ahmadi Ashtiani A, Faraji S, Amjad Iranagh S, Faraji AH. The study of electroless Ni-P alloys with different complexing agents on Ck45 steel substrate. Arabian J Chem. 2017;10:S1541–5. doi: 10.1016/j.arabjc.2013.05.015.
[26] Kadhim KN, Al-Rufaye AHR. The effects of uniform transverse magnetic field on local flow and velocity profile. Int J Civil Eng Tech (IJCIET). 2016;7(2):140–51.
[27] Ahmed JK. Improvement the hardness and wear of (Zn-Ni) coating layer by adding silicon carbide. Iraqi J Mech Material Eng. 2011;11(3):526–40.
[28] Srivastava M, WilliamGrips VK, Rajam KS. Influence of SiC, Si3N4 and Al2O3 particles on the structure and properties of electrodeposited Ni. Materials Letters. 2008;62(20):3487–9. doi: 10.1016/j.matlet.2008.03.008.